INDEX COPERNICUS INTERNATIONAL



Bio-Algorithms and Med-Systems

WWW.BAMSJOURNAL.COM ISSN: 1896-530X

ORIGINAL ARTICLE

Received: 14.08.2024
Accepted: 27.12.2024
Published: 27.12.2024

CITE THIS ARTICLE AS:
Dinari A, Ahmad HA, Bui MP, Oh S, Kim Y-H, Kim D-H, Yoon J, "Targeted Cellular Tracking of Pancreatic Cancer Cells via Magnetic Particle Spectroscopy (MPS)" Bio-Algorithms and Med-Systems vol. 20, special issue, pp. 63-70, 2024, DOI: 10.5604/01.3001.0054.9363

AUTHORS' CONTRIBUTION:
A. Conceptualization
B. Data Curation
C. Formal Analysis
D. Funding Acquisition
E. Investigation
F. Methodology
G. Project Administration
H. Resources
I. Software
J. Supervision
K. Validation
L. Visualization
M. Writing – Original Draft
N. Writing – Review & Editing

CORRESPONDING AUTHOR:
Jungwon Yoon; School of Integrated Technology, Gwangju Institute of Science and Technology, Gwangju 61005, Republic of Korea; E-mail: jyoon@gist.ac.kr

COPYRIGHT:
Some rights reserved: Jagiellonian University Medical College. Published by Index Copernicus Sp. z o. o.

OPEN ACCESS:
The content of the journal „Bio-Algorithms and Med-Systems" is circulated on the basis of the Open Access which means free and limitless access to scientific data.

CREATIVE COMMONS CC BY:
Attribution. It is free to copy, distribute, present and perform the copyrighted work and derivative works developed from it, provided that the name of the original author is cited.

Targeted Cellular Tracking of Pancreatic Cancer Cells via Magnetic Particle Spectroscopy (MPS)

Ali Dinari[1ACEFMN], Hafiz Ashfaq Ahmad[1BFN], Minh Phú Bùi[1I], Seungjun Oh[1I], Yun-Hee Kim[2G], Dae-Hong Kim[2BFGKN], Jungwon Yoon[1DGN]

[1]School of Integrated Technology, Gwangju Institute of Science and Technology, Gwangju, Republic of Korea
[2]National Cancer Center, Goyang-si, Gyeonggi-do, Republic of Korea

ABSTRACT

Objective: Pancreatic cancer is an asymptomatic disease and, based on statistical studies, it is the fourth leading cause of cancer-related death. Pancreatic ductal adenocarcinoma (PDAC), which accounts for over 95% of pancreatic cancers, is typically detectable at advanced stages. Standard diagnostic methods include blood-based tests and imaging. Standard diagnostic methods include blood-based tests and imaging. Biomarkers play a key role as indicators in blood tests, offering valuable insights into disease detection and monitoring. Mesothelin, a cell-surface glycoprotein, and vimentin, an intermediate filament protein, are promising biomarker candidates.
Methods: In this study, these biomarkers were conjugated with magnetic nanoparticles (MNPs) and utilized for cellular tracking through magnetic particle spectroscopy (MPS). Capan-1 (a pancreatic cancer cell line) and bone marrow stem cells (BMSC) were treated with the targeted MNPs. Subsequently, MNP-labelled cells were evaluated with imaging modalities such as MPS and confocal microscopy.
Results: In the case of the MPS modality, a home-made MPS device with a detection limit of 1 ng of MNPs was used. The results showed that MPS can quantitatively trace MNPs signals and differentiate between various treatments.
Conclusions: Detection of labelled cells via MPS is a novel method with features such as sensitivity, non-invasiveness, and no background noise. This new technology can pave the way for imaging quantification of pancreatic cancer in its primary stages and for tracking cancer cell populations. populations.

KEYWORDS

cellular tracking, pancreatic cancer, mesothelin, vimentin, magnetic particle spectroscopy

LIST OF ABBREVIATIONS

Ant-M-MNPs – anti-mesothelin-MNPs
Ant-V-MNPs – anti-vimentin-MNPs
BMSCs – bone marrow stem cells
CT – computerised tomography
DLS – dynamic light scattering
mAbs – anti-vimentin monoclonal antibodies
MES – (2-(N-Morpholino) ethanesulfonic acid hydrate, 4-Morpholineethanesulfonic acid
MNPs – magnetic nanoparticles
MPI – magnetic particle imaging
MPS – magnetic particle spectroscopy
MRI – magnetic resonance imaging
PBS – phosphate buffered saline
PDAC – pancreatic ductal adenocarcinoma
PDI – polydispersity index
PET – positron emission tomography

BRIEF DESCRIPTION OF THE WORK

This study introduces a novel, highly sensitive method using magnetic particle spectroscopy (MPS) for tracking pancreatic cancer cells. By detecting labelled cells with minimal background noise, this technology offers a promising approach for early diagnosis and monitoring of pancreatic cancer, potentially improving outcomes in clinical practice.

INTRODUCTION

Cancer research studies have shown that pancreatic cancer is a highly fatal malignancy and is projected to become the second leading cause of cancer-related death in the U.S. population within the next 20 to 30 years [1]. The most prevalent type of pancreatic cancer is ductal adenocarcinoma (PDAC). The symptoms associated with pancreatic cancer are often vague, similar to symptoms caused by other cancer types, and may not be present in the early stages of disease [2]. It is often diagnosed at an advanced stage [3]. Heterogeneity in tumour mass and tumour biomarkers has resulted in poor prognosis. The standard and non-invasive methods for diagnosis of pancreatic cancer are biomarker-based blood tests and imaging modalities [4]. An important aspect of imaging is focused on tracking the fate of cancerous cells. The ability to track tumour cell populations is a powerful tool for diagnosis and therapy in the early stages of many cancer types [5], and such tracking is reliant on the use of biomarkers. In this regard, mesothelin, a cell-surface glycoprotein with normal expression limited to mesothelial cells showed a high level of expression in the case of PDAC [6]. Vimentin, another candidate for predicting pancreatic cancer, is a filament-like protein that plays an essential role in protecting cells against stress [7]. Leveraging biomarkers like mesothelin and vimentin in conjunction with MNPs can enable the development of targeted MNPs for tracking pancreatic cancer cells. Imaging quantification through modalities such as MPS and magnetic particle imaging (MPI) are new approaches and represent a superior sensitivity compared to MRI and optical imaging [8]. In this research, in vitro experiments were conducted to evaluate the capability of MPS in tracing MNPs within MNP-labelled cells. The Capan-1 cell line and BMSCs were treated with plain MNPs and conjugated MNPs, including anti-mesothelin-MNPs (Ant--M-MNPs) and anti-vimentin-MNPs (Ant-V-MNPs). The treated cells were assessed using an MPS device to trace the MNPs' signals, with the detection of these signals serving as a precise indicator for distinguishing the effects of different treatments on the aforementioned cells. Through this approach, it is demonstrated that the quantification ability of the MPS modality could provide a new method for tracking cancer cell populations and advancing imaging technologies in biology and medicine.

MATERIALS AND METHODS

Florescent magnetic nanoparticles (F-MNPs, code: 126-01-501) were purchased from Micromod company (GmbH, Germany). The 1-Ethyl-3-(3-dimethylaminopropyl) carbodiimide (EDC, CAS No: 25952-53-8), N-Hydroxysuccinimide (NHS, CAS No, 6066-82-6) and 4',6-Diamidino-2-phenylindole dihydrochloride, 2-(4-Amidinophenyl)-6-indolecarbamidine dihydro-chloride (DAPI, CAS No, number: 28718-90-3) were purchased from Sigma-Aldrich (South Korea). Monoclonal antibodies including anti-mesothelin (CAS No: 13128-MM01), and anti-vimentin (CAS No: 100254-R001) were purchased from Sino Biological (Beijing, China). The pancreatic cancer cell line named Capan-1 was purchased from Korean Cell Bank (Seoul, South Korea). Mesenchymal stem cells-bone marrow (BMSC) (Cat. No: 10MU-042) were prepared from iXCells Biotechnologies company (San Diego, USA). RPMI 1640 Medium (cat number; 11875093) was purchased from Thermo Fisher Scientific (USA). MSC-specific cell mediums (Cat: MD-0003b and MD-0037) were purchased from iXCells Biotechnologies (USA).

Conjugation of biomarkers on the MNP

Mesothelin (14.7 μM) and vimentin (18.18 μM) were conjugated to the F-MNPs (5 mg/mL). In brief, using the EDC-NHS conjugation protocol, anti-mesothelin and anti-vimentin monoclonal antibodies (mAbs) were added to individual tubes (1.5 mL) containing plain MNPs. The ratio between MNPs and proteins was 1:5 respectively. To keep this ratio fixed, the applied concentration of MNPs per mAbs was 5 mg/mL / 0.44 μM. The conjugation process was performed in an MES buffer with the pH adjusted to 6. The reaction agents, including the MES buffer, MNPs, mAbs, and EDC-NHS powders, were added to the reaction tubes, pipetted twice at a 15-minute interval, and shaken at 50 RPM for 2 hours. Next, the reaction tubes were placed on magnetic beads for 24 hours and then washed with PBS to separate the conjugated proteins from the unreacted ones. The washing step was repeated three times to ensure the removal of unreacted proteins. Finally, to confirm the conjugation of proteins on the protein on the MNP, FT-IR spectroscopy and dynamic light scattering (DLS) were used. In this regard, the FT-IR spectrum of each sample was obtained

via an FT-IR (Perkin Elmer, Frontier, USA) spectrometer after mixing with KBr powder. In the next step, the hydrodynamic size and zeta potential of conjugated MNPs were evaluated by DLS measurements (Malvern Pananalytical, Malvern, UK). To conduct DLS analysis, the conjugated MNPs were washed three times and then dispersed in PBS (pH 7.4). The final concentration of the conjugated MNPs in the PBS solution was 100 µg/mL.

Cell culture

The Capan-1 cell line and BMSC were cultivated according to standard protocols. In this regard, 1×10^5 cells were seeded into T25 flasks in both cases (Capan-1 and BMSCs). The mediums, including RPMI 1640 (Thermo Fisher Scientific, USA) and MSC Growth Medium 2 (iXCells Biotechnologies, USA), were used as the culture media for treating Capan-1 and BMSC cells, respectively. The culture media were replaced every 2 or 3 days, and cells were kept sub-confluent according to each cell line's maintenance protocol.

Cellular tracking and imaging quantification

To track the conjugated MNPs in the desired cells, modalities such as confocal microscopy and the MPS device were applied. At a confluency of over 80%, the cells were treated with F-MNPs for 30 minutes, after which a fresh complete medium was added and the cells were incubated for 12 hours [9, 10]. The treatments, including plain MNPs, Ant-M-MNPs, and Ant-V-MNPs, were applied at the same concentration. To hinder experimental errors, each treatment was repeated three times. The initial concentration of conjugated MNPs in stock was 2 mg/mL, and the final concentration in the medium surrounding the cells was 50 µg/mL. A total volume of 2 mL of medium was applied to each confocal dish, whereas 5 mL of medium was used to treat the MPS experiment samples in each T25 flask. The volumes of applied conjugated-MNPs were 50 µl for the confocal dish and 125 µL for the T25 flask respectively. Hence the final concentration of MNPs in the cell medium was approximately 50 µg/mL. Indeed, to select the appropriate concentration of MNPs (50 µg/mL) and incubation time (12 hours), previous research provided valuable guidance. It is shown that iron oxide nanoparticles have low toxicity at concentrations below 100 µg/mL the application of cell cultures. However, this level can be vary based on the particle size, shape, charge, and exposure conditions. In general, the toxicity rages of MNPs, are divided into three categories: minimal toxicity (1–50 µg/mL), moderate toxicity (50–100 µg/mL), and high toxicity (>100 µg/mL) [11, 12]. With regard to time scales for the incubation of cells with MNPs, the characteristics of MNPs (size, shape, coating etc.) and the intended application (drug delivery / imaging applications) can have effects on the results. Regarding the time schedule, short incubation (1–5 hours), moderate incubation (12–24) and extended incubation (48–72 hours) are applied in research. In the case of short incubation, the purpose of nanoparticle uptake is investigated. In moderate incubation, the same objective is applied to ensure that internalisation can be completed efficiently. In the case of extended incubation, the therapy aim is the goal. However, extended exposure may increase the cytotoxic effects, especially at higher concentrations [9, 10]. In this research, the goal was to achieve the optimum nanoparticles uptake while preventing any toxic effect on the cells. Therefore, a 12-hour incubation period was selected for the moderate incubation time in order to increase the rate of uptake while inhibiting the potentially toxic effect of MNPs on cells.

Confocal microscopy imaging

To conduct confocal microscopy experiment, the cells were seeded in a specific confocal dish (Cat. No: 104350, glass bottom 100350). The cultivated cells on the confocal dish surface were washed with PBS (three times), fixed using 4% paraformaldehyde, and stained with DAPI (1 µg/mL). Images were obtained using a confocal laser scanning microscope (FV3000RS, Olympus, Tokyo, Japan).

MPS analysis experiment

In the case of MPS investigation, the experiments were conducted by culturing the cells in a T25 flask. At 80% confluency, the cells were treated with F-MNPs for 30 minutes, after which a fresh complete medium was added and the cells were incubated for 12 hours. Following this, the cell medium was removed, and the cells were detached and centrifuged. In the final step, the isolated cells were placed in the homemade MPS device's coil and the recorded signals were collected.

RESULTS AND DISCUSSION

Advanced imaging technologies in biology and medicine are developing with numerous innovations. Many sophisticated detection schemes have emerged for the diagnosis of cancer, based on imaging modalities including MRI, computerised tomography (CT), positron emission tomography (PET), and optical imaging techniques such as fluorescence and confocal microscopy [13]. However, in the case of precise detection, many challenges remain unmet [14]. For example, in the case of pancreatic cancer, the current modalities cannot detect it in its early stages. In this research, the detection of pancreatic cancer cell populations was evaluated using biomarker-targeted MNPs and a homemade MPS device (Fig. 1.). Through the application of MPS technology and tracking of MNPs, a collection of quantitative data was obtained, indicating that MPS technology has the potential to be used in nanomedicine as a new modality for the detection of pancreatic cancer.

Conjugation of biomarkers on the MNP surfaces

The characterisation of conjugated MNPs was evaluated using FT-IR and DLS devices, and the accuracy of the conjugation process was confirmed and is shown in Fig. 2. Related to the FT-IR spectrum, the peaks located at 580 cm^{-1} and 625 cm^{-1} were ascribed to the stretching vibration mode of Fe–O bonds in Fe_3O_4 [15]. The peak that appeared at 1520 cm^{-1} corresponds to the NH_2 bending vibration, indicating the presence of functional groups on the MNPs' surface [16]. The peak appeared at

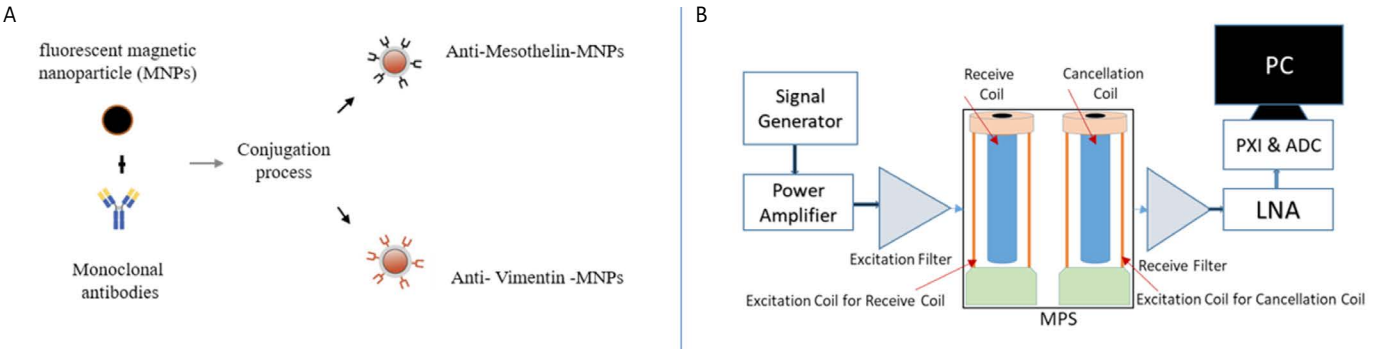

Fig. 1. (A) Schematic representation of the conjugation process of magnetic nanoparticles (MNPs) with monoclonal antibodies to produce targeted Anti-Mesothelin-MNPs and Anti-Vimentin-MNPs for specific cell recognition; (B) Schematic diagram of the Magnetic Particle Spectroscopy (MPS) setup, including signal generation, excitation and receive coils, cancellation coil, and data acquisition system for precise detection and measurement of MNP signals.

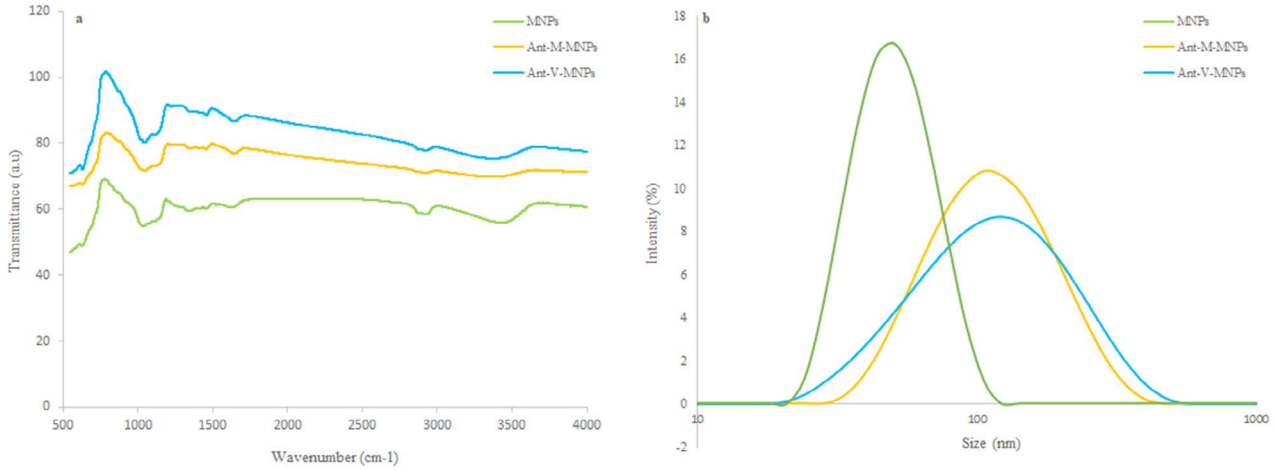

Fig. 2. (A) FT-IR spectra of MNPs, Anti-M-MNPs, and Anti-V-MNPs, showing characteristic absorption bands that confirm the successful conjugation of antibodies; (B) DLS analysis illustrating the size distribution of MNPs, Anti-M-MNPs, and Anti-V-MNPs, with slight increases in particle size indicating antibody functionalisation.

865 cm^{-1} in the spectrum of conjugated MNPs and its absence in plain MNPs can be ascribed to the C-O-H group, which represents the carboxyl groups of the amino acids in the protein backbone [17]. The characteristic peak at a wavenumber of 1240 cm^{-1} is attributed to the C-N group belonging to proteins (mesothelin and vimentin).

DLS analysis also confirmed the accuracy of the conjugation process. The measured average sizes of plain MNPs, Ant-M--MNPs, and Ant-V-MNPs were nearly 50 nm, 125 nm, and 133 nm, respectively. Indeed, due to antibodies being attached to the MNPs' surfaces, the hydrodynamic size increased. The zeta potential analysis, which monitors the surface charge of MNPs, can confirm the conjugation process [18, 19]. The MNPs are covalently bound to the carboxyl groups (-COOH) of the monoclonal antibodies (mAbs). Hence, the surface charge of the entire system (mAbs--MNPs) became negative. In the case of plain MNPs, the surface charge is positive due to the presence of NH_2 groups on the MNPs' surface. The conjugation of proteins to MNPs shifts the zeta potential towards negative values (Tab. I.).

In fact, the zeta potential can indicate the stability of conjugated MNPs. As shown in Tab. I. the parameters of size (intensity--based), polydispersity index (PDI), and zeta potential are recorded. Regarding the three different MNPs – the plain NPs, mesothelin--conjugated MNPs, and vimentin-conjugated MNPs – the presented data show differences in their properties. According to the table, the zeta potential of plain plain MNPs is approximately 11 mV.

Tab. I. DLS analysis of conjugated MNPs, showing the average values from three independent measurements.

SAMPLES	INTENSITY (nm)	PDI	ZETA POTENTIAL (mV)
Plain MNPs	51.65	0.083	11.33
Mesothelin-conjugated MNPs	120.8	0.235	–5.37
Vimentin-conjugated MNPs	129.93	0.29	–5.17

However, due to the conjugation process, it shifts to lower values (≈ –5 mV) in the case of conjugated MNPs. Previous studies indicated that plain MNPs with a zeta potential of > +30 or < –30 are relatively stable, whereas those with a zeta potential between +15 and –15 are unstable [18–20]. In this study, the stability of conjugated plain MNPs was not the focus of investigation. In fact, the conjugated MNPs were prepared one day prior to treating the cells of interest. As a recommended good practice, the tubes containing MNPs were carefully pipetted to prevent precipitation in the solvent before being added to the cell medium. It is also worth mentioning that published papers indicate that these conjugated MNPs can remain stable at 2–8°C (refrigerator temperature) for up to a month [21, 22].

Cellular Tracking and Imaging Quantification

A plausible commonest approach to perceiving the dynamics of cellular events is perhaps that of live cell imaging, which relies on light microscopy techniques [23]. Optical imaging has the advantages of high spatial and temporal resolution, high sensitivity, and low cost in use. However, the main obstacle of optical imaging is its weakness in penetration and access to deep layers of tissues and organs. Scatter and absorbance of light within the tissue limited is to a few millimetres below the tissue [24]. Another drawback of optical imaging is the lack of quantification in the obtained data. On the other hand, magnetic-based imaging, including MRI, MPI, and MPS with novel advantages are considerable. Non-invasiveness and non-radiation characteristics make them very promising candidates for molecular imaging and cellular tracking with the ability to image the depth tissues [25, 26]. Tracking the fate of iron-labelled cells with minimum effects on cell activities has been investigated through MRI and significant achievements have been recorded [27]. Despite its importance in clinical medicine as the most powerful technique for disease tracking and monitoring, MRI still faces challenges in achieving highly sensitive and quantitative cell tracking. In this regard, the low specificity of MRI is the outcome of low-signal regions (air-filled lungs or haemorrhage sites) in the images, and also the signal void volume does not have a linear relation with the number of cells, which resulted in complexity of quantification of the iron-induced signal losses [5, 28]. In contrast to MRI, both MPI and MPS focus solely on tracing MNP signals, regardless of background noise. In this research, the ability of MPS technology as a zero-dimensional MPI was evaluated through in vitro experiments, demonstrating its capability to detect MNPs in target cells (Capan-1 and BMSC) regardless of tissue background noise. The results showed that MPS technology has superiority over confocal microscopy. Specifically, MPS technology can provide quantitative data and illustrate differences in cellular uptake with various MNP treatments. As shown in Fig. 3., the confocal microscopy results displayed similar patterns of cellular uptake across different MNP treatments, making it difficult to distinguish between the uptake rates of plain and conjugated MNPs. The limitations, particularly in quantifying images and differentiating MNP concentrations within target cells, are due to the qualitative nature of the data. However, the MPS data shown in Fig. 4. clearly demonstrate the differences across the various treatments.

In the Capan-1 cell line, the difference is clearly shown, with the highest signals observed for M-MNPs, followed by V-MNPs. Cell uptake of M-MNPs and V-MNPs is significantly higher than that of plain MNPs, indicating that the targeting strategy was effective. Another notable difference is observed between treatments of Ant-M-MNPs and Ant-V-MNPs. Since Capan-1 cells are epithelial and express more mesothelin than vimentin, it is expected that the data show stronger signals for Ant-M-MNPs compared to Ant-V-MNPs [6, 29, 30]. However, in the case of BMSCs, which are mesenchymal stem cells, higher signals from Ant-V-MNPs are expected [7, 31]. This indicates that MSCs express higher levels

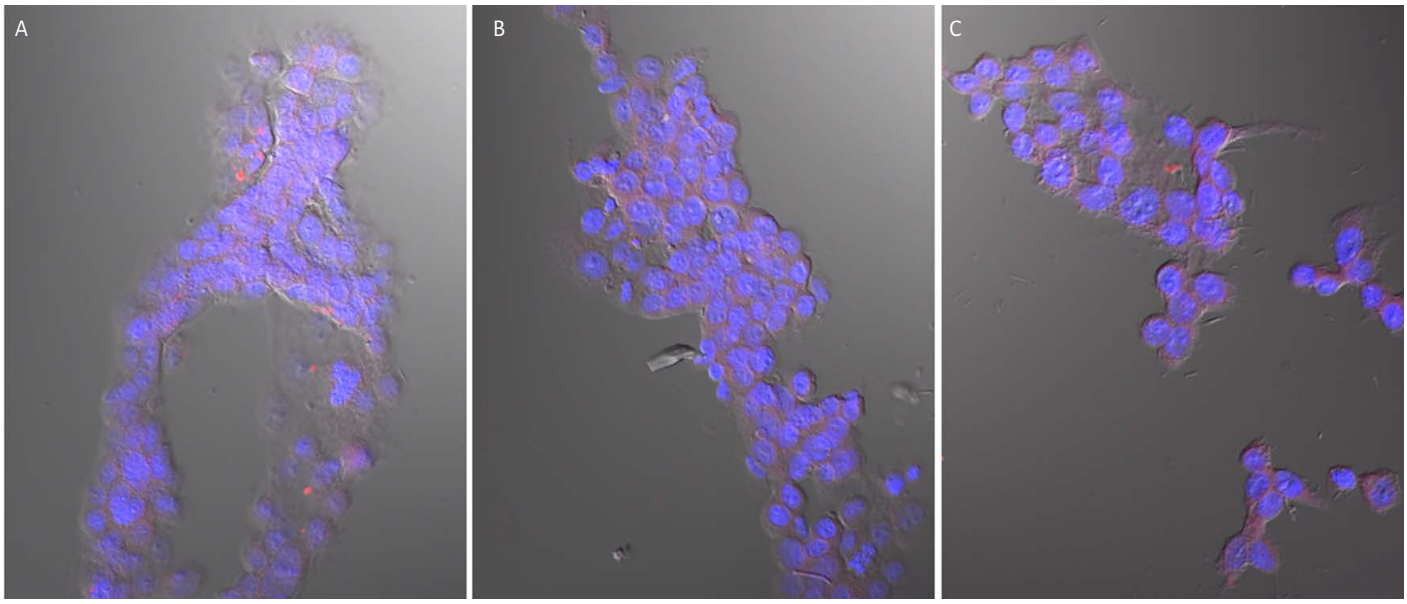

Fig. 3. Confocal Microscopy Results: Images of Capan-1 cells treated with fluorescent MNPs show distinct treatments: (A) plain MNPs; (B) Ant-M-MNPs, and (C), and Ant-V-MNPs. Cell nuclei are stained blue (DAPI dye), while MNPs appear as a reddish-pink fluorescence.

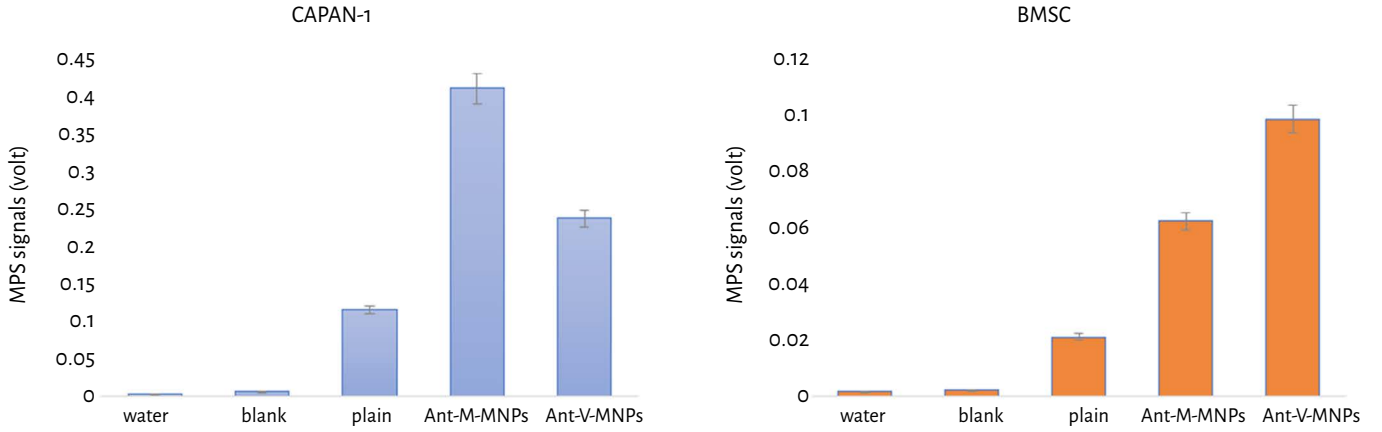

Fig. 4. MPS signals recorded from the Capan-1 cell line (left) and BMSCs (right). In Capan-1 cells, the highest uptake was observed with Ant-M-MNPs, while in BMSCs, the highest uptake was with Ant-V-MNPs. Water and blank samples (cells without MNPs) served as controls.

of vimentin, suggesting that vimentin-targeted MNPs could be a more effective strategy for tracking MSCs.

Another significant finding is the difference in MNP uptake between Capan-1 and BMSCs, as presented in Fig. 5. Analysis of MPS signal data from both Capan-1 and BMSCs, reveals differences in MNPs cell uptake. Capan-1 cells, being cancerous, exhibit distinct metabolic processes and interactions with MNPs compared to BMSCs. As expected, cancerous cells consume more energy and metabolites than normal BMSCs. The MPS data support this expectation, indicating varying levels of exogenous material uptake. In BMSCs, a normal cell type, material trafficking and metabolism are tightly regulated. In contrast, Capan-1 cells display abnormalities in membrane trafficking and metabolism [32–34]. In fact, the rate of MNP uptake in Capan-1 cells is high, which is due to upregulated endocytosis pathways in tumour cells, resulting in more efficient uptake [35]. It is noteworthy that the retention time of NPs inside the cells can generally range from several hours to a few days [35]. For example, gold NPs or silica NPs can be retained inside cells for 1–3 days, especially if they are not actively cleared through exocytosis or lysosomal degradation [36]. In the case of MNPs, they are often retained inside cells for 1–7 days or even longer, depending on the MNPs surface modifications, the cellular uptake mechanism and the cell's ability to degrade or excrete them [37]. Factors such as size, coating and surface modification of MNPs can influence their retention time. Research on biodegradable polymer-coated MNPs found that they were retained in cancer cells for approximately 48–72 hours before being degraded [38]. PEGylation or coating with polymers such as chitosan or dextran can extend the retention time due to stabilisation of the NPs and reduced clearance [39]. Antibody functionalisation for targeted delivery can also enhance the uptake and retention in specific cell types, such as cancer cells. The NH2-functionalised dextran-coated MNPs conjugated with anti-mesothelin and anti-vimentin, as applied in this research study, are biocompatible with a composition of cross-linked dextran-iron oxide composite particles. They are stable in aqueous buffers with pH > 4, and suspension in a PBS buffer (pH = 7.4).

As presented in the results of this article, both Capan-1 and BMSCs cells could uptake them. However, the rate of uptake is different [40]. A study on MNP uptake and retention in HeLa cells showed that the NPs were retained for up to 6 days without significant exocytosis [41]. Similarly, other studies have demonstrated similar retention times in different cell types. Capan-1 cells exhibit similar behaviour to HeLa cells. On the other hand, MSCs show retention of MNPs ranging from several days to weeks, which is beneficial for applications like cell tracking [39]. BMSCs can take up nanoparticles through endocytosis, though the rate may be lower compared to cancer cells. These cells are more likely to retain nanoparticles if the particles are designed to interact specifically with the cell membrane or intracellular structures [40].

An interesting convergence application that can be integrated with the approach of this study is combining it with magnetic hyperthermia for the treatment of PDAC. In fact, a research study that uses MPI as feedback to guide magnetic hyperthermia treatments over several days has been performed (nanorobotics group, GIST, South Korea) [42]. MNPs were injected directly into the tumour and hyperthermia was performed. In fact, the intertumoral injection is the last option and will always be applied in the final steps when the other options have failed. MPI enables daily monitoring of tumour size, showing a gradual reduction. If tumour persistence is detected, a precise amount of MNPs can be re-injected, and hyperthermia applied until the tumour is eradicated. Additionally, MPI is used to estimate the remaining amount of MNPs within the tumour area each day, enabling optimised planning of subsequent injections for complete treatment. Indeed, MPI can determine the location of MNPs accurately. However, for in vitro investigations, MPS is preferred due to its higher sensitivity. It is noteworthy that intravenous injection is always challenging due to several issues, such as elimination, capture by blood immune cells, and scavenging by reticuloendothelial cells. By using MPS and MPI technology, it is possible to trace the smallest amount of MNPs. Given a sufficiently effective targeting of MNPs to reach the PDAC lesion and cancerous cells, their detection in this region could serve as an indicator of PDAC disease. Therefore,

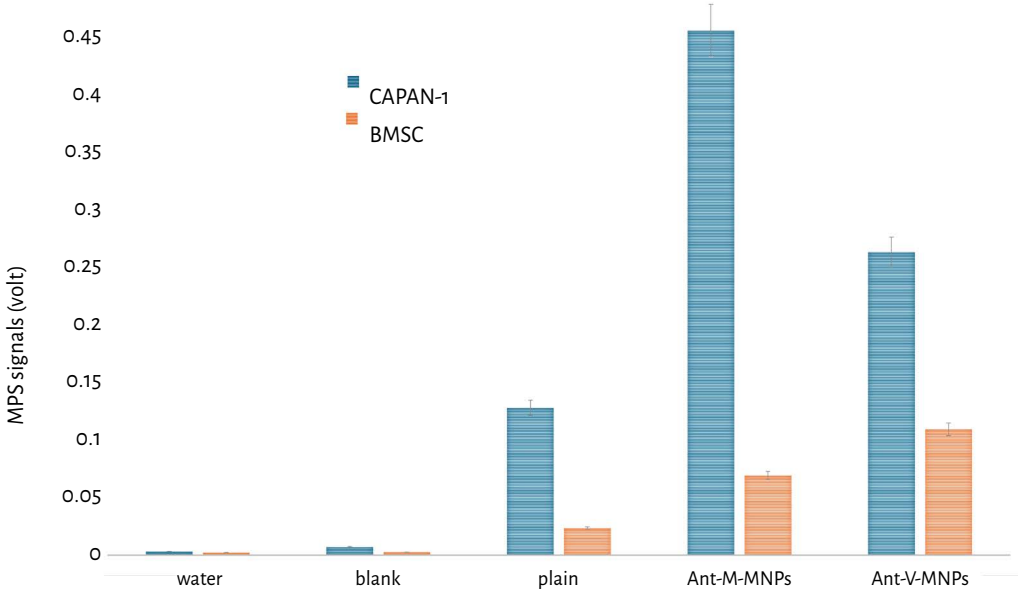

Fig. 5. Comparison of MPS signals from Capan-1 cells and BMSCs, showing distinct uptake levels. As illustrated in the figure, nanoparticle interactions and uptake differ significantly between cancerous and normal cells.

in order to reach this goal the intravenous injection issues must be overcome. Even though bioconjugate MNPs, in combination with MPS/MPI technology (for imaging and diagnostic purposes), have the potential to be utilised in primary diagnosis and in preventing the extension of lesion sites, the injection issue must be addressed for optimal performance.

Overall, the expression of these two candidates in pancreatic cancer is feasible, and targeting MNPs with these proteins could be an effective strategy for tracking pancreatic cancer tumour cells [43]. The outcome of this study suggests that MPS technology, combined with conjugated MNPs, could be a valuable approach for pancreatic cancer detection. Ultimately, this strategy could pave the way for new research utilising MPS and MPI as non-invasive, yet highly sensitive and precise technologies for diagnosing cancer in its early stages.

CONCLUSIONS

This study successfully demonstrated the potential of MPS as a highly sensitive and non-invasive modality for tracking the magnetic labelled cells. By conjugating MNPs with biomarkers such as mesothelin and vimentin, the tracking of the pancreatic cancer cells (Capan-1) and bone marrow stem cells (BMSCs) was evaluated. It is evident that this study did not directly evaluate the detection of pancreatic cancer cells, but it has enough potential to be used for that purpose. The results revealed that MNP-based cellular tracking via MPS technology could differentiate between various cell treatments, providing quantitative data and highlighting the effectiveness of MPS--based diagnosis. The targeted MNPs displayed distinct patterns of cellular uptake, with mesothelin-conjugated MNPs showing stronger signals in Capan-1 cells and vimentin-conjugated MNPs showing higher uptake in BMSCs, consistent with their respective biomarker expressions. These findings suggest that MPS, in combination with targeted MNPs, could be a powerful tool for cellular tracking and diagnosis approaches. This strategy has the potential to be applied as a new non-invasive cancer diagnostic method and to impact clinical practices through precise detection and tracking of cancerous cells and tumour progression.

CONFLICT OF INTEREST

Authors have declared no potential conflicts of interest.

REFERENCES

1. McGuigan A, Kelly P, Turkington RC, Jones C, Coleman HG, McCain RS. Pancreatic cancer: A review of clinical diagnosis, epidemiology, treatment and outcomes. World J Gastroenterol. 2018;24(43):4846.
2. Mizrahi JD, Surana R, Valle JW, Shroff RT. Pancreatic cancer. Lancet. 2020;395(10242):2008–20.
3. Park W, Chawla A, O'Reilly EM. Pancreatic cancer: a review. JAMA. 2021;326(9):851–62.
4. Kaur S, Baine MJ, Jain M, Sasson AR, Batra SK. Early diagnosis of pancreatic cancer: challenges and new developments. Biomark Med. 2012;6(5):597–612.
5. Sehl OC, Foster PJ. The sensitivity of magnetic particle imaging and fluorine-19 magnetic resonance imaging for cell tracking. Sci Rep. 2021;11(1):22198.
6. Zervos E, Agle S, Freistaedter AG, Jones GJ, Roper RL. Murine mesothelin: characterization, expression, and inhibition of tumor growth

in a murine model of pancreatic cancer. J. Exp. Clin. Cancer Res. 2016;35:1–13.

7. Green KJ, Böhringer M, Gocken T, Jones JC. Intermediate filament associated proteins. Adv. Protein Chem. 2005;70:143–202.
8. Tay ZW, Chandrasekharan P, Fellows BD, Arrizabalaga IR, Yu E, Olivo M, et al. Magnetic particle imaging: An emerging modality with prospects in diagnosis, targeting and therapy of cancer. Cancers. 2021;13(21):5285.
9. Malhotra N, Lee J-S, Liman RAD, Ruallo JMS, Villaflores OB, Ger T-R, et al. Potential toxicity of iron oxide magnetic nanoparticles: a review. Molecules. 2020;25(14):3159.
10. Namvar F, Rahman HS, Mohamad R, Baharara J, Mahdavi M, Amini E, et al. Cytotoxic effect of magnetic iron oxide nanoparticles synthesized via seaweed aqueous extract. Int J Nanomedicine. 2014:2479–88.
11. Soenen SJ, Rivera-Gil P, Montenegro J-M, Parak WJ, De Smedt SC, Braeckmans K. Cellular toxicity of inorganic nanoparticles: common aspects and guidelines for improved nanotoxicity evaluation. Nano Today. 2011;6(5):446–65.
12. Kim D-K, Zhang Y, Voit W, Rao K, Kehr J, Bjelke B, et al. Superparamagnetic iron oxide nanoparticles for bio-medical applications. Scr. Mater. 2001;44(8–9):1713–7.
13. Huntosova V, Andreana M, Unterhuber A. Advanced imaging and its application in biology and medicine. Front Cell Dev Biol. 2023 Mar 8;11:1163210.
14. Kastelik-Hryniewiecka A, Jewula P, Bakalorz K, Kramer-Marek G, Kuźnik N. Targeted PET/MRI imaging super probes: a critical review of opportunities and challenges. Int J Nanomedicine. 2022 Jan 1:16:8465–8483.
15. Fekri Aval S, Akbarzadeh A, Yamchi MR, Zarghami F, Nejati-Koshki K, Zarghami N. Gene silencing effect of SiRNA-magnetic modified with biodegradable copolymer nanoparticles on hTERT gene expression in lung cancer cell line. Artif Cells Nanomed Biotechnol. 2016;44(1):188–93.
16. Wang X, Lin KS, Chan JC, Cheng S. Direct synthesis and catalytic applications of ordered large pore aminopropyl-functionalized SBA-15 mesoporous materials. J. Phys. Chem. B 2005;109(5):1763–9.
17. Chafidz A, Astuti W, Augustia V, Novira DT, Rofiah N. Removal of methyl violet dye via adsorption using activated carbon prepared from Randu sawdust (Ceiba pentandra). Bristol: IOP Conference Series: Earth and Environmental Science; IOP Publishing; 2018.
18. Honary S, Zahir F. Effect of zeta potential on the properties of nano-drug delivery systems-a review (Part 1). Trop. J. Pharm. Res. 2013;12(2):255–64.
19. Honary S, Zahir F. Effect of zeta potential on the properties of nano-drug delivery systems-a review (Part 2). Trop. J. Pharm. Res. 2013;12(2):265–73.
20. Bhattacharjee S. DLS and zeta potential–what they are and what they are not? J. Control. Release. 2016;235:337–51.
21. Arami H, Khandhar AP, Tomitaka A, Yu E, Goodwill PW, Conolly SM, et al. In vivo multimodal magnetic particle imaging (MPI) with tailored magneto/optical contrast agents. Biomaterials. 2015;52:251–61.
22. Stiufiuc GF, Stiufiuc RI. Magnetic Nanoparticles: Synthesis, Characterization, and Their Use in Biomedical Field. Appl. Sci. 2024;14(4):1623.
23. Stephens DJ, Allan VJ. Light microscopy techniques for live cell imaging. Science. 2003;300(5616):82–6.
24. Foy SP, Manthe RL, Foy ST, Dimitrijevic S, Krishnamurthy N, Labhasetwar V. Optical imaging and magnetic field targeting of magnetic nanoparticles in tumors. ACS Nano. 2010;4(9):5217–24.
25. Sehl OC, Gevaert JJ, Melo KP, Knier NN, Foster PJ. A perspective on cell tracking with magnetic particle imaging. Tomography. 2020;6(4):315–24.
26. Zhang W, Liang X, Zhu L, Zhang X, Jin Z, Du Y, et al. Optical magnetic multimodality imaging of plectin-1-targeted imaging agent for the precise detection of orthotopic pancreatic ductal adenocarcinoma in mice. EBioMedicine. 2022;80:104040.
27. Tremblay M-L, O'Brien-Moran Z, Rioux JA, Nuschke A, Davis C, Kast WM, et al. Quantitative MRI cell tracking of immune cell recruitment to tumors and draining lymph nodes in response to anti-PD-1 and a DPX-based immunotherapy. Oncoimmunology. 2020;9(1):1851539.
28. Lazaro-Carrillo A, Filice M, Guillén MJ, Amaro R, Viñambres M, Tabero A, et al. Tailor-made PEG coated iron oxide nanoparticles as contrast agents for long lasting magnetic resonance molecular imaging of solid cancers. Mater Sci Eng C Mater Biol Appl. 2020;107:110262.
29. Weekes CD, Lamberts LE, Borad MJ, Voortman J, McWilliams RR, Diamond JR, et al. Phase I study of DMOT4039A, an antibody–drug conjugate targeting mesothelin, in patients with unresectable pancreatic or platinum-resistant ovarian cancer. Mol. Cancer Ther. 2016;15(3):439–47.
30. Hassan R, Thomas A, Alewine C, Le DT, Jaffee EM, Pastan I. Mesothelin immunotherapy for cancer: ready for prime time? J. Clin. Oncol. 2016;34(34):4171–9.
31. Mittal V. Epithelial mesenchymal transition in tumor metastasis. Annu. Rev. Pathol. 2018;13(1):395–412.
32. Fu X, Liu G, Halim A, Ju Y, Luo Q, Song G. Mesenchymal stem cell migration and tissue repair. Cells. 2019;8(8):784.
33. Bergers G, Fendt S-M. The metabolism of cancer cells during metastasis. Nat. Rev. Cancer. 2021;21(3):162–80.
34. Sneeggen M, Guadagno NA, Progida C. Intracellular transport in cancer metabolic reprogramming. Front Cell Dev Biol. 2020;8:597608.
35. Samanta K, Setua S, Kumari S, Jaggi M, Yallapu MM, Chauhan SC. Gemcitabine combination nano therapies for pancreatic cancer. Pharmaceutics. 2019;11(11):574.
36. Chen Y, Hou S. Recent progress in the effect of magnetic iron oxide nanoparticles on cells and extracellular vesicles. Cell Death Discov. 2023;9(1):195.
37. Sakhtianchi R, Minchin RF, Lee K-B, Alkilany AM, Serpooshan V, Mahmoudi M. Exocytosis of nanoparticles from cells: role in cellular retention and toxicity. Adv. Colloid Interface Sci. 2013;201:18–29.
38. Meyer RA, Green JJ. Biodegradable polymer iron oxide nanocomposites: the future of biocompatible magnetism. Nanomedicine (Lond). 2015;10(23):3421–5.
39. Bulte JW, Douglas T, Witwer B, Zhang S-C, Strable E, Lewis BK, et al. Magnetodendrimers allow endosomal magnetic labeling and in vivo tracking of stem cells. Nat. Biotechnol. 2001;19(12):1141–7.
40. Ren R, Tan X-H, Zhao J-H, Zhang Q-P, Zhang X-F, Ma Z-J, et al. Bone marrow mesenchymal stem cell-derived exosome uptake and retrograde transport can occur at peripheral nerve endings. Artif Cells Nanomed Biotechnol. 2019;47(1):2918–29.
41. Popescu R, Savu D, Dorobantu I, Vasile B, Hosser H, Boldeiu A, et al. Efficient uptake and retention of iron oxide-based nanoparticles in HeLa cells leads to an effective intracellular delivery of doxorubicin. Sci. Rep. 2020;10(1):10530.
42. Le T-A, Hadadian Y, Yoon J. A prediction model for magnetic particle imaging–based magnetic hyperthermia applied to a brain tumor model. Comput. Methods Programs Biomed. Update. 2023;235:107546.
43. Wei T, Zhang X, Zhang Q, Yang J, Chen Q, Wang J, et al. Vimentin-positive circulating tumor cells as a biomarker for diagnosis and treatment monitoring in patients with pancreatic cancer. Cancer Lett. 2019;452:237–43.